Photonic molecules doped with semiconductor nanocrystals

B. M. Möller and U. Woggon*
Fachbereich Physik, Universität Dortmund, Otto-Hahn-Strasse, 4, 44227 Dortmund, Germany

M. V. Artemyev
Institute for Physico-Chemical Problems of Belarussian State University, Minsk 220080, Belarus

R. Wannemacher
Fakultät für Physik und Geowissenschaften, Universität Leipzig, Linnéstrasse 5, D-04103 Leipzig, Germany
(Received 22 June 2004; published 24 September 2004)

We report on coherent cavity field coupling in linear chains and arrays of exactly size-matched spherical microcavities doped with CdSe quantum dots. The spatial distribution and the dominant polarization type of both the weakly and strongly coupled cavity resonances are studied spectrally and spatially resolved in various coupled resonator geometries. Both experiment and theory show strong photon mode coupling with pronounced mode splitting as well as weak coupling with no significant loss in *Q*-factor depending on the emitter position and orientation.

DOI: 10.1103/PhysRevB.70.115323 PACS number(s): 73.22.−f, 78.67.−n, 78.70.−g, 42.70.−a

I. INTRODUCTION

Optical microcavities trapping light into three-dimensionally confined photon modes attract substantial interest in the field of cavity quantum electrodynamics (CQED) and light-matter interaction.[1–4] In particular, the combination with quasi zero-dimensionally confined electronic structures, e.g., semiconductor quantum dots, has been established as a promising material system in optoelectronics and photonics.[5,6] For applications of spherical microcavities in low-threshold lasers[7,8] or coupled-resonator optical waveguides,[9] cavities with high optical finesse $Q=\omega/\Delta\omega$, small mode volume, and well-defined emission patterns are highly desirable. Until now the implementation of preferred symmetry axes for directional emission of sphere-based cavities has been realized by shape distortion of the resonator[10] while more complex coupled-sphere geometries are less studied. Confinement of light in multisphere-based photonic molecules might open a way to optimize cavity parameters by creation of a more complex cavity structure than a single microsphere. Photonic molecule formation based on coupling of photonic dots is reported for dye-doped polymeric bisphere systems[11] and laterally patterned planar microresonators containing quantum wells as the optically active medium.[12] Recently, the preparation of controlled, symmetrical multisphere agglomerations by wet-chemical means has been reported in Refs. 13 and 14 suggesting the possibility of three-dimensional photonic molecules and microscale optical manipulation applications. Likewise, an interesting type of optical waveguide is proposed in Ref. 9 that consists of a sequence of coupled microdisk or microsphere cavities that provides lossless and reflectionless bending of photons. Lasing of a coherently coupled bisphere system is recently described in Ref. 15.

In this paper we study coherently coupled microsphere cavities doped with CdSe nanocrystals. The spatial distribution and polarization properties of both the weakly and strongly coupled cavity fields are studied spectrally and spatially resolved in various one- and two-dimensional multisphere geometries. The experimental data are compared with a calculation of field distributions and mode linewidths as a function of dipole orientation and position inside a photonic molecule. We demonstrate *Q*-factor conservation for weakly coupled and field concentration along molecule axes for strongly coupled modes as important properties of coupled resonator geometries. The combination of polarization-sensitive mode mapping and spectral analysis at characteristic symmetry points of the molecule allowed us the identification of weakly and strongly coupled bonding and antibonding modes and the determination of the dominant polarization type of the molecule states.

II. SAMPLES AND EXPERIMENT

The photonic molecules were prepared by impregnating polystyrene microspheres (Polysciences, Inc., radius $R \approx 1.4\ \mu$m, refractive index $n \approx 1.59$) with a subsurface layer of CdSe nanocrystals (NCs) of $R_{NC}=2.5$ nm according to Ref. 16. After synthesis of CdSe nanocrystals following Ref. 17, the methanolic suspension of microspheres was cast and dried on a quartz substrate thereby forming a great variety of microsphere assemblies. To achieve coherent photon coupling, exactly size-matched microspheres ($<0.1\%$ size deviation) have been preselected via their Mie resonances. The photonic molecule modes are studied by microphotoluminescence spectroscopy at the diffraction limit combined with polarization-sensitive mode mapping. The spectra and the spatial intensity distribution are taken with a spatial resolution of 0.4 μm and a spectral resolution of 0.2 nm at room temperature. The intensity of NC-doped spheres is spectrally and spatially resolved by mapping the intensity across a sphere on and off resonance to molecule modes for a fixed polarization plane. A polarizer inserted into the optical beam path in front of the detection system selects only signals from NCs that emit components of the electromagnetic field

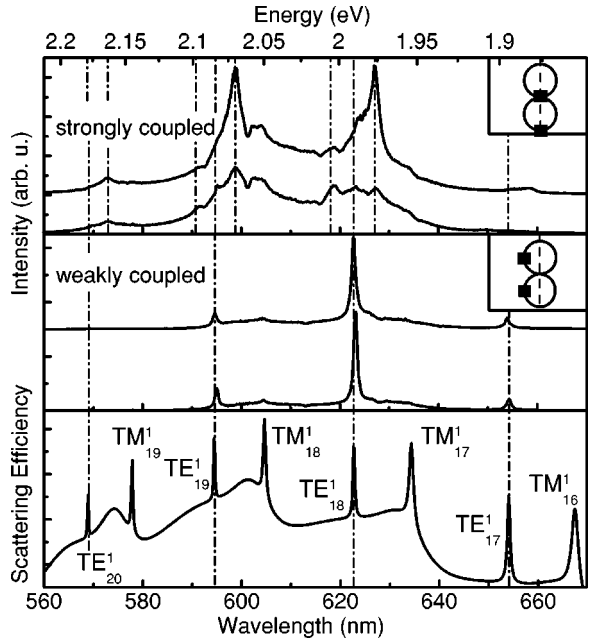

FIG. 1. Emission spectra taken in TE-sensitive detection (see text) at characteristic bisphere points. Upper panel: redshifted, bonding resonances measured at the intersection point (uppermost curve) and weaker, antibonding modes taken at the edge position; middle panel: spectra of the spectrally unshifted bisphere modes taken at detection points apart from the bisphere axis; lower panel: Mie-scattering spectrum for a single polystyrene sphere.

parallel to the orientation of the polarizer. In that way we can reduce the total mode spectrum into subsets of either TE- or TM-like modes for more clarity in the data analysis (for experimental details see Refs. 6 and 18. By the narrow spectral window and the chosen polarizer orientation, we introduce a size selection of NCs from the inhomogeneously broadened ensemble that are exactly in resonance to the investigated cavity mode and have components of the optical transition dipole moment according to the field orientation defined by the polarizer axis.

III. PHOTONIC MOLECULES FORMED BY TWO COUPLED MICROSPHERE CAVITIES

The simplest photonic molecule is a coherently coupled bisphere system which implements a preferred symmetry axis along the molecule axis. We, therefore, start with the analysis of bisphere emission spectra and field intensity distributions, which are excited here by the emission of CdSe nanocrystals near the surface of the microspheres. Figure 1 shows the emission spectra taken at characteristic detection points of a bisphere molecule, i.e., on- and off-axis with respect to the bisphere axis. The lower panel shows, for comparison, the scattering spectrum for a single sphere calculated via standard Mie theory. The labels TE_{ℓ}^{n} or TM_{ℓ}^{n} denote the polarization type (TE or TM) and the angular (ℓ) and radial (n) quantum numbers, respectively. For the analysis of the spectra we select in the following only one subset of either TE- or TM-types modes by using a polarization sensitive detection. For example, the data in Fig. 1 are detected as TE-sensitive by orienting the axis of a linear polarizer parallel to the bisphere axis for off-axis detection at the equator and perpendicular for on-axis detection at the pole.

For detection points off-axis near the equators (middle panel), the single-sphere TE resonance energies, e.g., the TE modes with $n=1$ and $\ell=17$, 18, 19, are well reproduced in the spectrum of the bisphere system. Because of the negligible spectral shift compared to the single-sphere TE-resonances, the mode type excited by nanocrystals at off-axis positions is called *weakly coupled* throughout this paper without further classification into bonding and antibonding modes. Spectra taken at the on-axis detection points (upper panel) show the characteristic mode splitting caused by coherent mode coupling, as has been demonstrated in Ref. 11. These strongly coupled resonances can be classified in bonding or antibonding modes with the help of the intensity maps and by comparing the absolute intensity at the intersection region of the bisphere with the intensity at its end positions (see Fig. 2). Based on the experimental data we identify the redshifted mode at 627 nm (uppermost curve in Fig. 1) as a pronounced bonding mode because of its high signal at the intersection point compared to the upper and lower on-axis detection points.

The polarization-sensitive and spectrally resolved intensity maps of both the spectrally unshifted, weakly coupled, and spectrally redshifted, strongly coupled modes are shown in Fig. 2. To extract the dominant polarization of the respective mode type, the intensity maps are again decomposed in TE and TM contributions by changing the orientation of the linear polarizer in the detection beam path. We found that in a linearly aligned sphere geometry (see also Fig. 4), the single-sphere polarization character of the discrete photon states survives to a major extent. The color-coded maps show the polarization-sensitively detected spatial intensity distributions in resonance to a weakly coupled [Fig. 2(b) and 2(c)] and a strongly coupled, bonding TE-like mode [Fig. 2(d)]. In case of the weakly coupled modes, the detected signal is almost vanishing along the bisphere axis, indicating a weak cavity field at these regions originating from intersphere coupling. The intensity map for the strongly coupled mode, on the other hand, (here spectrally shifted by 5 nm, see Fig. 1) exhibits the inverse intensity distribution compared to Fig. 2(c), showing a signal only at those positions where the weakly coupled modes have no intensity. By comparing to Fig. 1 we see that the respective spectra are characterized by sharp peaks with no significant broadening in case of the weakly coupled modes of Figs . 2(b) and 2(c) and by split-off, spectrally broader peaks for the strongly coupled mode of Fig. 2(d).

To understand the influence of coherent photon coupling on the cavity field distribution and mode line shape, a comparative calculation of a bisphere system has been performed using the semianalytical MMP technique with systematic variation of dipole position, frequency, and orientation. The result is given in Fig. 3 for bisphere parameters of $R=1.3895$ μm radius and refractive index $n=1.58876$. We modeled here a *single* dipole emitter aligned in x direction and located in case (a) at $r=1.2$ μm from the center of the lower microsphere at the equator or in case (b) on the bi-

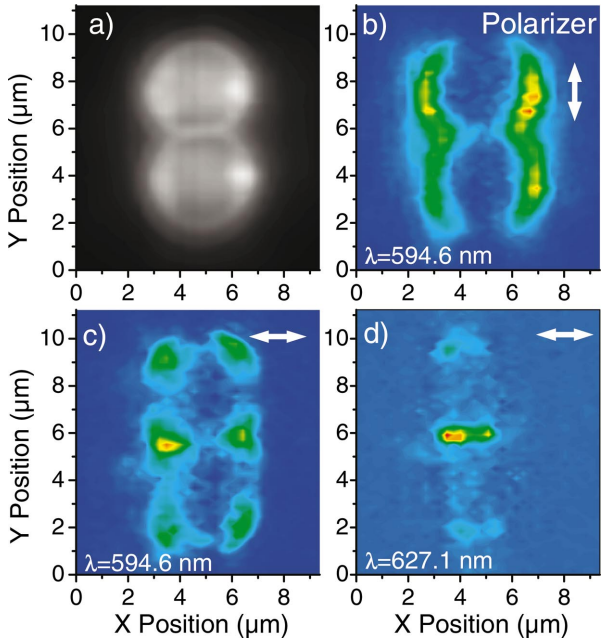

FIG. 2. (Color) Polarization-sensitive intensity maps of a bisphere photonic molecule for a weakly coupled TE_{19}-type resonance (b) and (c) and a strongly coupled bonding TE_{18}-type resonance (d) (note the stronger intensity in the bisphere center compared to that at the poles indicating the bonding type of the mode). The orientation of the polarizer is given by arrows. In (a) the spectrally integrated, unpolarized emission is shown. For the spectral positions see Fig. 1.

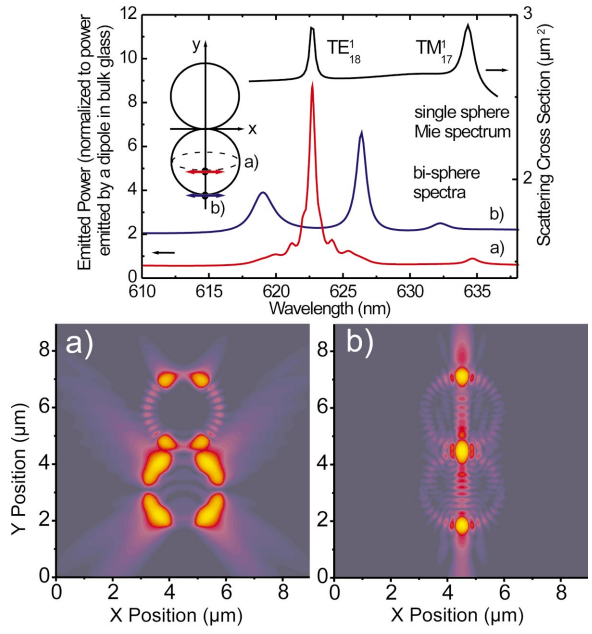

FIG. 3. (Color) Calculated emission spectrum and electric field intensity distributions $|E|^2$ excited by a dipole oscillating in x direction and (a) located in the lower sphere 1.2 μm from the center at the equator and (b) at the pole on the bisphere axis (see scheme in the inset). The upper panel shows the spectra, the lower panel the $|E|^2$-distribution in xy plane in a logarithmic color-coded scale of 40 dB. Spectrum (b) has an offset of +1.5 for clarity.

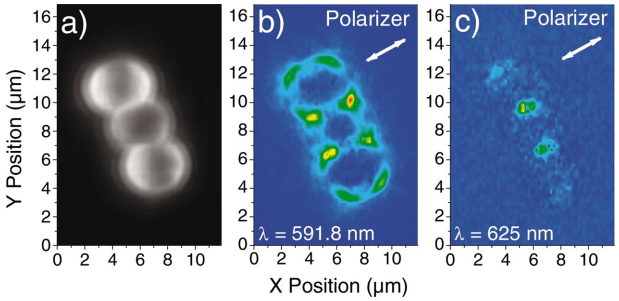

FIG. 4. (Color) Polarization-sensitive intensity maps of a trisphere linear chain configuration. The intensity distribution of a TE_{18}-type mode reveals similar characteristics compared to the bisphere system: vanishing intensity of the weakly coupled modes along the trisphere axis (b), complementary emission pattern of the strongly coupled bonding mode (c). The used polarization for the mode mapping is indicated by arrows.

sphere axis (see scheme in the inset of Fig. 3). The calculation for the bisphere system identifies the measured vanishing field intensity along the bisphere axis as a real, spatial, single-mode modification in a weakly coupled bisphere system without significant spectral mode shift and broadening [Fig. 3, case (a), marked in red] compared to the single-sphere spectrum. Both experiment and theory also show, for the strongly bonding modes, an increase in linewidth due to the additional loss mechanism caused by the strong intersphere coupling and a concentration of electric field intensity in three points along the bisphere axis [Fig. 3, case (b), marked in blue]. As can be seen from Figs. 1–3, we can

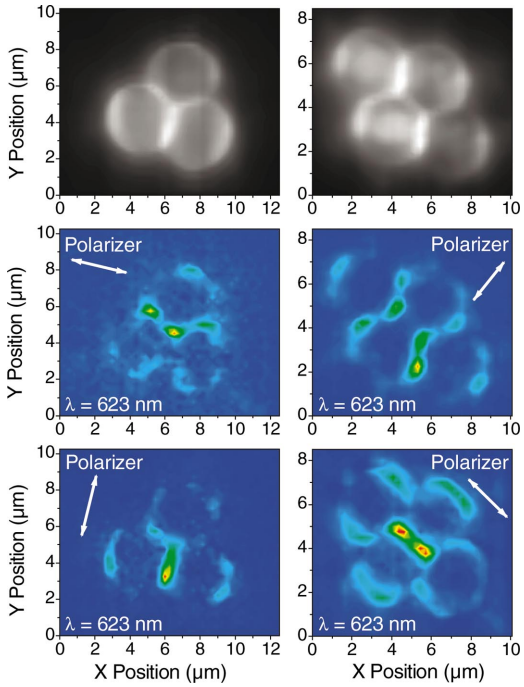

FIG. 5. (Color) Intensity characteristics of bonding resonances of triple (left) and quadruple (right) sphere configurations. In the first row the spectrally integrated intensity distributions are plotted, the other images show the intensity distribution for different polarizations of the mode mapping as indicated by arrows.

correlate the experimental mode mapping for weakly coupled (off-axis points) and strongly coupled (on-axis points) mode pictures with the calculated electromagnetic field intensity $|E|^2$ for tangential dipole orientation. The calculated spectra confirm the observation of coherent cavity coupling for resonant photons in exactly size-matched microcavities. Typical features are the conservation of the *Q*-factor for weak coupling, modification of the field intensity along the bisphere axis, and strong mode splitting in the strong coupling case.

Moreover, the calculation of the field distribution reveals a feature not present for single spheres: the mode excited at 632 nm in case (b) is a TM-type antibonding mode evolving from the TM_{18}-type single microsphere mode. While TM-type mode excitation is almost forbidden for tangentially aligned dipoles in an isolated sphere;[6] this mode type can obviously be more easily excited in a molecule. Details of the full-dipole orientation dependence of $|E|^2$ will be discussed in a forthcoming publication.

IV. LINEAR CHAIN GEOMETRIES OF COUPLED MICROSPHERE CAVITIES

The study of structures with more than two coupled cavities is motivated by our interest in waveguiding through weak coupling between high-*Q* optical cavities (the so-called CROW structure: coupled resonator optical waveguide).[9] This type of waveguiding might replace waveguiding by total internal reflection and waveguiding through Bragg reflection from a periodic structure. A particularly appealing feature of the CROW is the possibility of making lossless and reflectionless bends. The experimental realization requires polar geometries, such as microdisks or microspheres. With Fig. 4 we demonstrate, as a first step toward a CROW structure based on microspheres, the realization of a three-resonator coupling without significant *Q*-factor degrading.

As can be seen in Fig. 4, a linear chain consisting of three touching spheres shows exactly the characteristics found before in the bisphere system: weakly coupled TE-type modes have vanishing intensity along the trisphere axis while strongly coupled TE bonding modes exhibit strongest emission at touching points and split in red- and blueshifted modes (spectra not shown here). For the weakly coupled modes (off-axis positions), we measure no significant change in the *Q*-factor ($Q \sim 1000$) for either the bisphere or the linear three-sphere configuration, which is a promising result with respect to future application in weakly coupled, high-*Q* CROW-structures.

V. TWO-DIMENSIONAL GEOMETRIES OF COUPLED MICROSPHERE CAVITIES

Next, we studied the effect of next-neighbor and long-distance coupling by analyzing several two-dimensional sphere geometries. We focused on the stability of the photonic molecule formation while continuously including further constituents. This procedure can be considered as nothing but a bottom-up approach toward a two-dimensional (2D)-photonic structure and results in arrangements of symmetrical three- and four-sphere geometries. Figure 5 shows the spatially resolved emission intensity of a molecule state for two 2D-sphere configurations. As the main difference with respect to one-dimensional, linear chain geometries, we observe a redistribution of field intensity within the array toward the air gaps. As can be seen in Fig. 5, the strongest emission is detected close to the air-gap positions and not at the intersection points—in contrast to the strongly coupled resonances in linear tri-sphere geometries. This strong intensity localization at positions apart from the intersection points is only observed for geometries which deviate from the linear chain. To explain the pronounced intensity patterns at the air-gap positions in our multisphere configurations of Fig. 5, we propose a coherent three-sphere coupling. An argument for a complete coherent three-sphere coupling and not pairwise coupled two-sphere systems, is the fact, that an incoherent intensity sum would never vanish at the intersection points. These findings strongly support the term tight-binding coupling in which next-neighbor species have necessarily to be all included in the molecule formation, but distant objects have negligible effects. The addition of a fourth sphere did not significantly modify the spatial confinement at the center of the molecule. This fact, combined with the spectral features, highlights the feasibility of this photonic chemistry approach for new cavity designs.

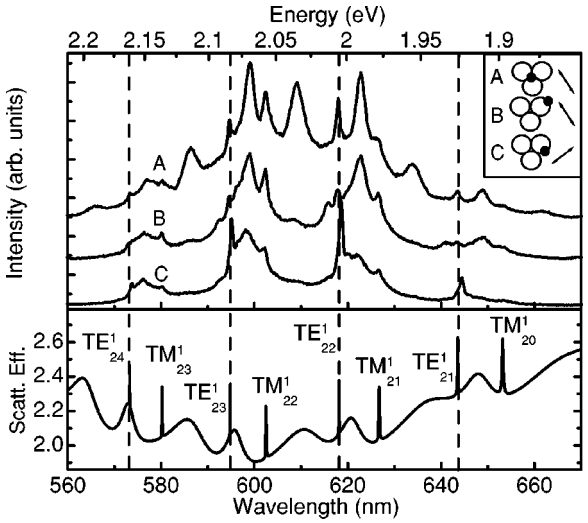

FIG. 6. Emission spectra taken at symmetry-relevant detection points for a trisphere system (see inset). The used polarization for detecting the spectra is indicated by arrows; lower panel: Mie scattering spectrum for a corresponding single polystyrene sphere.

The strong field intensity modification for molecules is evaluated more quantitatively by integrating the mapped intensity patterns in agglomerates and comparing it with the single-sphere case. We discuss the interesting case of weak coupling because the spatial modification of the emission intensity here is not accompanied with a large spectral broadening. The measured intensity distribution is integrated for maps of such weakly coupled modes taken at identical excitation and detection conditions for the same TE-type resonance. For off-axis positions we measure *Q*-values of 1200, 920, and 1000 for the single-sphere, bisphere, and 2D trisphere geometry, respectively. For the latter configuration,

the spectra at three symmetry-relevant positions are shown in Fig. 6, with the sharpest mode observed at the detection point C. The experimentally determined integrated mapped intensities normalized to the single-sphere case are $V_{\text{integr}} = 1$, 0.54, and 0.5 for the three configurations, resulting in an increase of the characteristic quantity Q/V_{integr} from 1 (single sphere) to 1.42 (bisphere) and 1.66 (2D trisphere).

VI. SUMMARY

In conclusion, we demonstrated the photonic molecule formation in one- and two-dimensionally coupled exactly size-matched microspheres and studied the spatial dependence and polarization type of both the weakly coupled and strongly coupled resonances. The comparison of different molecule geometries clearly showed a tight-binding coupling signature of the bonding photon states. The interference effects of the weakly coupled modes might be used to build a new type of structured cavity with easily modified light concentration in highly tunable systems. Both experiment and theory show that weak coupling, e.g., of three coupled resonators, with no significant loss in the *Q*-factor can be achieved as well as strong coupling with strong field concentration along the molecule axes. We hope that in future experiments the additional polarization control by changing the shape of the nanocrystals allows additional variations and control of photons.

Financial support of this work by the DFG in the form of Wo477/18, the EU RTN Project HPRN-CT-2002-00298, and INTAS 01/2100 is gratefully acknowledged.

*Electronic address: ulrike.woggon@uni-dortmund.de

[1] *Optical Processes in Microcavities*, edited by R. K. Chang and A. J. Campillo, Advanced Series in Appl. Physics Vol. 3 (World Scientific, Singapore, 1996).

[2] *Confined Photon Systems*, edited by H. Benisty, J. M. Gerard, R. Houdre, J. Rarity, and C. Weisbuch, Lecture Notes in Physics 531 (Springer-Verlag Berlin, 1999).

[3] T. Gutbrod, M. Bayer, A. Forchel, P. A. Knipp, T. L. Reinecke, A. Tartakovskii, V. D. Kulakovskii, N. A. Gippius, and S. G. Tikhodeev, Phys. Rev. B **59**, 2223 (1999).

[4] J. R. Buck and H. J. Kimble, Phys. Rev. A **67**, 033806 (2003).

[5] J. M. Gerard and B. Gayral, Physica E (Amsterdam) **9**, 131 (2001).

[6] U. Woggon, R. Wannemacher, M. V. Artemyev, B. Möller, N. LeThomas, V. Anikeyev, and O. Schöps, Appl. Phys. B: Lasers Opt. **77**, 469 (2003).

[7] S. Spillane, T. Kippenberg, and K. Vahala, Nature (London) **415**, 621 (2002).

[8] H. Schniepp and V. Sandoghdar, Phys. Rev. Lett. **89**, 257403 (2002).

[9] A. Yariv, Y. Xu, R. K. Lee, and A. Scherer Opt. Lett. **24**(11), 711 (1999).

[10] S. Lacey, H. Wang, D. H. Foster, and J. U. Nöckel, Phys. Rev. Lett. **91**, 033902 (2003).

[11] T. Mukaiyama, K. Takeda, H. Miyazaki, Y. J. Jimba, and M. Kuwata-Gonokami, Phys. Rev. Lett. **82**, 4623 (1999).

[12] V. Zhuk, D. V. Regelman, D. Gershoni, M. Bayer, J. P. Reithmaier, A. Forchel, P. A. Knipp, and T. L. Reinecke, Phys. Rev. B **66**, 115302 (2002).

[13] M. D. Barnes, S. M. Mahurin, A. Mehta, B. G. Sumpter, and D. W. Noid, Phys. Rev. Lett. **88**, 015508 (2002).

[14] V. N. Manoharan, M. T. Elsesser, and D. J. Pine, Science **301**, 483 (2003).

[15] Y. Hara, T. Mukaiyama, K. Takeda, and M. Kuwata-Gonokami, Opt. Lett. **28**, 2437 (2003).

[16] B. Möller, U. Woggon, M. V. Artemyev, and R. Wannemacher, Appl. Phys. Lett. **83**, 2686 (2003).

[17] D. V. Talapin, A. L. Rogach, A. Komowski, M. Haasse, and H. Weller, Nano Lett. **1**, 207 (2001); M. A. Hines and P. Guyot-Sionnest, J. Phys. Chem. **100**, 468 (1996); C. B. Murray, D. J. Norris, and M. G. Bawendi, J. Am. Chem. Soc. **115**, 8707 (1993).

[18] B. Möller, M. V. Artemyev, U. Woggon, R. Wannemacher, Appl. Phys. Lett. **80**, 3253 (2002).